

# Medical Image Classification Based on Transformer Model and Ordinal Loss

Yan Liu <sup>a</sup>

*School of Electronics Engineering and Computer Science, Peking University, Beijing, China*

**Keywords:** Medical Image Classification, ViT, Loss Function, Ordinal Regression.

**Abstract:** This study centers on the application of transformer models for general medical image classification, a crucial step towards automating medical diagnostics. By comparing transformer models with classical methods across diverse medical image datasets, this research aims to enhance performance on specific tasks within these datasets. The core model, Medical Vision Transformer (MedViT), effectively learns multi-scale features by integrating convolutional layers with specialized transformer modules, thereby catering to various medical image classification tasks across different categories. Moreover, this study introduces Ordinal Loss to augment the model's performance on ordinal regression subtasks. Unlike conventional cross-entropy loss, Ordinal Loss facilitates improved learning of sequential relationships between categories. Experiments conducted on MedMNIST validate that MedViT surpasses classical methods on most datasets, with Ordinal Loss further enhancing performance on ordinal regression subtasks. Visual analysis also confirms that the new loss function aids the model in effectively discerning key differences between adjacent categories. This research demonstrates the feasibility of employing a general-purpose transformer model to address medical image classification challenges across multiple domains. Additionally, plug-and-play modules can be leveraged to optimize the model for specific tasks, underscoring its versatility and potential for broader application in medical diagnostics.


## 1 INTRODUCTION

Medical imaging classification is a crucial process in healthcare as it involves the automated analysis of medical images to identify and categorize various medical conditions. This process assists in diagnosing diseases, monitoring treatment progress, and facilitating early detection of abnormalities, which can significantly improve patient outcomes. By leveraging advanced algorithms, it enhances the precision and speed of interpretation, reducing the workload on radiologists and potentially lowering the rate of misdiagnosis. Overall, medical imaging classification serves as an essential tool in modern medicine, enabling more accurate and efficient patient care. In recent years, the development of convolutional neural networks has greatly aided the progress of computer-aided medical imaging classification (Lo, 2022; Hu, 2022; Yang, 2021).

Convolutional Neural Network (CNN) can learn key features from images effectively and represent a

crucial model architecture for image classification in computer vision. VGGNet demonstrated the importance of depth in CNN architectures, featuring up to 19 layers and achieving remarkable success in the ImageNet challenge (Simonyan, 2014). ResNet addresses the problem of degradation in network depth by introducing residual connections, winning the ImageNet challenge and profoundly influencing future research on deep learning architectures (He, 2016).

Transformer is a model originating from the field of natural language processing. Vision Transformer transforms images into tokens for classification, pioneering the use of transformers in computer vision (Dosovitskiy, 2020). Pooling-based Vision Transformer innovates by integrating learnable pooling operations into the transformer architecture, enabling it to dynamically adjust the resolution of feature maps and improve efficiency and performance across various vision tasks (Heo, 2021). Medical Vision Transformer (MedViT) is a kind of

<sup>a</sup> <https://orcid.org/0009-0000-9961-3162>

Vision Transformer model specifically designed for medical imaging tasks. It leverages the transformer's ability to capture global dependencies and complex patterns within images to improve the accuracy and efficiency of diagnosing and analyzing medical images (Manzari, 2023).

This study focuses primarily on utilizing MedViT for medical image classification tasks, with a comprehensive analysis of factors influencing its performance and subsequent enhancements. Addressing the challenge of limited dataset sizes, data augmentation techniques are deployed to augment the model's generalization capability. Moreover, to mitigate overfitting concerns, various model depths are explored through comparative experiments. In response to the performance limitations in ordered regression subtasks, a novel loss function termed ordinal loss is developed, directly applicable to the model. Comparative experiments between ordinal loss and the original model are conducted, with results visualized using interpretable models. The findings indicate that MedViT offers a significant advantage over classical methods, and the newly designed loss function effectively enhances the model's performance in ordered regression subtasks. This study marks a notable progress in lightweight medical image classification, especially in tackling ordinal regression subtasks.

## 2 METHODOLOGIES

### 2.1 Dataset Description and Preprocessing

MedMNIST (Yang, 2023) is a lightweight, cross-domain medical image classification dataset structured similarly to MNIST. It comprises 12 types of 2D data and 6 types of 3D data. This study primarily experiments on the 12 types of 2D data, and their image types and labels are as follows:

PathMNIST consists of histopathological slices of colorectal cancer tissue, with dimensions of  $3 \times 28 \times 28$ , and includes labels for 9 types of tissue.

ChestMNIST consists of frontal-view X-ray images of the chest, with dimensions of  $1 \times 28 \times 28$ , and includes 14 disease labels, constituting a multi-label binary classification task.

DermaMNIST consists of dermatoscopic images, with dimensions of  $3 \times 28 \times 28$ , and includes labels for 7 types of pigmented skin diseases.

OCTMNIST consists of optical coherence tomography (OCT) images of the retina, with

dimensions of  $1 \times 28 \times 28$ , and includes labels for 4 diagnosis categories.

PneumoniaMNIST comprises pediatric chest X-ray images, with dimensions of  $1 \times 28 \times 28$ , constituting a binary classification task for pneumonia and healthy cases.

RetinaMNIST consists of retinal fundus images, with dimensions of  $3 \times 28 \times 28$ , forming a 5-level ordinal regression for diabetic retinopathy severity.

BreastMNIST consists of breast ultrasound images, with dimensions of  $1 \times 28 \times 28$ , forming a binary classification task for benign and malignant breast cancer.

BloodMNIST consists of microscope images of blood cells, with dimensions of  $3 \times 28 \times 28$ , comprising 8 labels.

TissueMNIST comprises microscope slice images of human kidney cortex cells, with dimensions of  $1 \times 28 \times 28$ , containing 8 different category labels.

OrganMNIST consists of CT images of human body organs from different orientations, with dimensions of  $1 \times 28 \times 28$ , and includes labels for 11 organ categories.

These datasets vary in size and encompass various subtasks of image classification. Random scaling, rotation, cropping, and horizontal flipping are employed as data augmentation techniques.

### 2.2 Proposed Approach

The original dataset provides benchmarking for some classical CNNs and AutoML methods on the 12 2D datasets, using accuracy (ACC) and area under the receiver operating characteristic (ROC) curve (AUC) as evaluation metrics. To compare the performance differences between MedViT and classical convolutional networks, a MedViT model is trained on the same datasets and evaluated using the same metrics. One of these datasets is RetinaMNIST, used for classifying retinal image lesion severity, which falls under ordinal regression tasks. Most models, including MedViT, generally get low ACC on this task. To address this, a new loss function (ordinal loss) with hyperparameters is designed to replace the original cross-entropy loss function and train it under different hyperparameters to compare its performance. Subsequently, the researcher selects the model with the greatest performance improvement and uses GradCAM for visual monitoring to visualize and analyze the effect of the new loss function on enhancing ordered regression tasks, validating the design concept. The entire experimental process is illustrated in Figure 1.

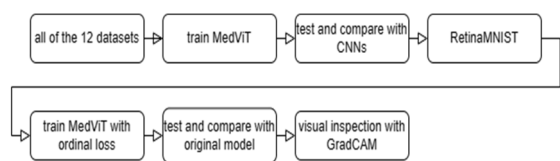


Figure 1: The pipeline of the research (Photo/Picture credit: Original).

### 2.2.1 MedViT

MedViT is a hybrid architecture of CNN and transformer. It contains two main modules, Local Transformer Block (LTB) and Efficient Convolution Block (ECB). Both modules contain a Locally Feed Forward Network (LFFN).

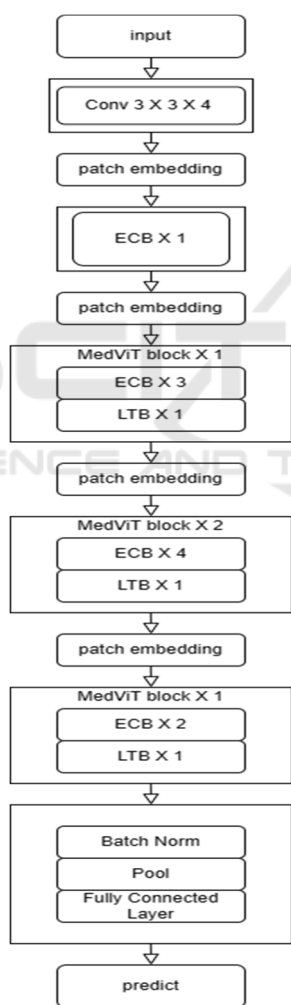


Figure 2: The architecture of MedViT (Photo/Picture credit: Original).

LFFN rearranges the token sequence into a 2D grid and performs convolution, then rearranges it back into a token sequence. In this way, it can capture

the locality information in the data. An ECB block is made by a multi-head convolution attention block and LFFN connected together. It is used to learn the long-range dependencies between pixels corresponding to the background. In an LTB, an improved version of the self-attention block is used to capture low-frequency signals, while the multi-head convolution attention block is used to capture high-frequency signals in different parallel representation subspaces. Their outputs are then concatenated to achieve a mix of high and low-frequency signals. The architecture of MedViT is shown in Figure 2 and the specific structure of LFFN, LTB and ECB are shown in Figure 3. A MedViT block consists of one or more ECB and LTB blocks stacked together. The image input passes through an initial convolutional layer and an ECB block. Then, it traverses through multiple sets of MedViT blocks of varying scales to comprehensively learn features at different scales. Finally, it goes through pooling and fully connected layers to obtain classification predictions. Given the smaller size of the data images, shallower model depths are employed to prevent overfitting. However, in other application scenarios, stacking more MedViT blocks can lead to improved performance.

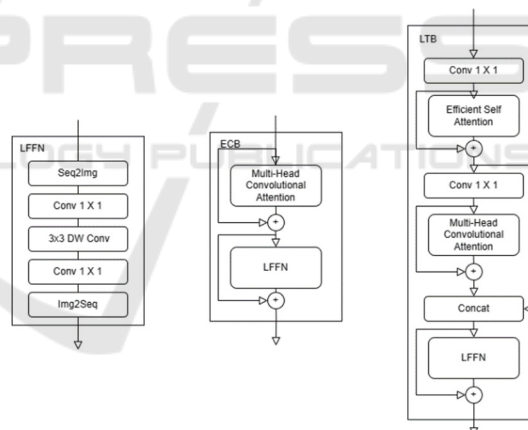


Figure 3: The structure of LFFN, LTB and ECB (Photo/Picture credit: Original).

### 2.2.2 GradCAM

Gradient-weighted Class Activation Mapping (GradCAM) is a technique utilized to visualize the significance of specific regions within an image for a neural network's predictions. It provides insights into the prediction process of the model by highlighting the portions of the input image that contribute most significantly to its prediction. Although GradCAM was initially developed for analyzing CNNs, it can also be applied to transformer models. Unlike when

applied to CNNs, where GradCAM typically utilizes the output and gradients from the last convolutional layer, when applied to transformer models, it generally leverages the output and gradients from the final transformer block. These gradients represent the importance of each feature map for the final prediction. Using these gradients, the contribution of each token to the classification result is calculated. These contributions are subsequently correlated with the spatial positions on the original image to generate a heatmap. Elevated values in the heatmap denote areas where the model concentrates its attention during predictions.

By overlaying this heatmap onto the input image, it can be visually interpreted which parts of the image are most important for the neural network's prediction. This can visually represent the process and basis of the model's classification.

### 2.2.3 Loss Function

Cross-entropy loss function measures the difference between two probability distributions: the predicted probability distribution output by the model and the true probability distribution of the labels. This loss function penalizes incorrect predictions more severely as their confidence increases, leading to more effective training of classification models. Cross-entropy loss function is commonly expressed as:

$$L_c = -\sum_{i=1}^N y_i \log \hat{y}_i \quad (1)$$

where  $N$  is the number of labels,  $y_i$  is the true probability (0 or 1) of the sample belonging to class  $i$ , and  $\hat{y}_i$  is the predicted.

This research designs a new loss function, Ordinal Loss, for addressing ordinal regression tasks. The motivation behind this design is that the loss function should optimize the model's output towards a unimodal distribution closer to the true probability distribution, while simultaneously enhancing the sensitivity between adjacent categories as much as possible. Ordinal Loss is calculated as:

$$\text{Margin Rank}(y_+, y_-, t) = \max(0, -t(y_+ - y_-) + \text{margin}) \quad (2)$$

$$\text{Rank Loss} = \sum_{i=0}^{N-1} \sum_{j=i+1}^N \text{Margin Rank}(\hat{y}_i, \hat{y}_j, t_{ij}), \quad (3)$$

$$t_{ij} = \begin{cases} 1, & \text{if label} > \frac{i+j}{2} \\ -1, & \text{otherwise} \end{cases} \quad (4)$$

$$\text{Ordinal Loss} = \alpha \text{Rank Loss} + (1 - \alpha)L_c \quad (5)$$

where  $\alpha$  is a hyperparameter, label is the true class of the sample, and margin is a parameter fixed at 0.1. It can be seen that Ordinal Loss is a combination of rank loss and traditional cross-entropy loss. The rank loss encourages the model's predicted probability distribution to approach a more realistic unimodal distribution, while also enhancing the sensitivity of the model to adjacent categories. As  $\alpha$  increases, the model's optimization direction becomes more influenced by the rank loss.

### 2.3 Implementation Details

The training is conducted on an Nvidia A800 GPU. The model is independently trained for 50 epochs on 12 datasets, with a batch size of 128. The learning rate is set to 0.001 at the beginning, adopting a cosine decay strategy over a cycle of 50 epochs. In the experimental section of ordinal loss, keeping other settings unchanged, training is conducted on RetinaMNIST, and is set to 0, 0.1, 0.2, 0.3, 0.4, and 0.5, respectively. All training is performed using the AdamW optimizer.

## 3 RESULTS AND DISCUSSION

The experimental results include the testing performance of MedViT on 12 datasets and the accuracy of MedViT with ordinal loss on RetinaMNIST. The comparison between MedViT's ACC and AUC on all 12 datasets and classical methods is illustrated in Table 1. MedViT performs exceptionally well on the PathMNIST dataset, with the highest AUC of 0.992 and a very high ACC of 0.909 compared to the other methods listed. This suggests MedViT is very effective at distinguishing between the different classes in this particular dataset. For the PneumoniaMNIST dataset, MedViT again has an impressive AUC of 0.978 and ACC of 0.939, outperforming all other methods by a notable margin in AUC, indicating strong performance in terms of the model's ability to rank predictions correctly. In the OCTMNIST, MedViT has good AUC and ACC scores, but not the highest. Its AUC of 0.960 and ACC of 0.783 are strong, but Google AutoML Vision has slightly better performance with an AUC of 0.963 and ACC of 0.771. MedViT's performance on the other datasets is also generally strong, often within the top three methods. For example, it performs very well on the BloodMNIST with an AUC of 0.997 and an ACC of 0.968, suggesting a high capability of distinguishing between classes accurately.

Table 1: Performance of MedViT and other classical methods on 12 datasets.

Methods	PathMNIST		ChestMNIST		DermaMNIST		OCTMNIST		PneumoniaMNIST	
	AUC	ACC	AUC	ACC	AUC	ACC	AUC	ACC	AUC	ACC
ResNet-18 (28)	0.983	0.907	0.768	0.947	0.917	0.735	0.943	0.743	0.944	0.854
ResNet-18 (224)	0.989	0.909	0.773	0.947	0.92	0.754	0.958	0.763	0.956	0.864
ResNet-50 (28)	0.99	0.911	0.769	0.947	0.913	0.735	0.952	0.762	0.948	0.854
ResNet-50 (224)	0.989	0.892	0.773	0.948	0.912	0.731	0.958	0.776	0.962	0.884
auto-sklearn	0.934	0.716	0.649	0.779	0.902	0.719	0.887	0.601	0.942	0.855
AutoKeras	0.959	0.834	0.742	0.937	0.915	0.749	0.955	0.763	0.947	0.878
Google AutoML Vision	0.944	0.728	0.778	0.948	0.914	0.768	0.963	0.771	0.991	0.946
MedViT	0.992	0.909	0.550	0.947	0.924	0.768	0.960	0.783	0.978	0.939
Methods	BreastMNIST		BloodMNIST		TissueMNIST		OrganAMNIST		OrganCMNIST	
	AUC	ACC	AUC	ACC	AUC	ACC	AUC	ACC	AUC	ACC
ResNet-18 (28)	0.901	0.863	0.998	0.958	0.93	0.676	0.997	0.935	0.992	0.900
ResNet-18 (224)	0.891	0.833	0.998	0.963	0.933	0.681	0.998	0.951	0.994	0.920
ResNet-50 (28)	0.857	0.812	0.997	0.956	0.931	0.68	0.997	0.935	0.992	0.905
ResNet-50 (224)	0.866	0.842	0.997	0.95	0.932	0.68	0.998	0.947	0.993	0.911
auto-sklearn	0.836	0.803	0.984	0.878	0.828	0.532	0.963	0.762	0.976	0.829
AutoKeras	0.871	0.831	0.998	0.961	0.941	0.703	0.994	0.905	0.99	0.879
Google AutoML Vision	0.919	0.861	0.998	0.966	0.924	0.673	0.99	0.886	0.988	0.877
MedViT	0.856	0.891	0.997	0.968	0.922	0.672	0.997	0.932	0.993	0.920

For the TissueMNIST dataset, MedViT's performance is not as strong as on other datasets, with an AUC of 0.922 and an ACC of 0.672. While the AUC is relatively high, the ACC is the lowest among the reported results for this dataset. For OrganMNIST datasets, MedViT maintains high AUC scores (0.997, 0.992, and 0.975 respectively) and high ACC (ACC scores of 0.932, 0.920, and 0.796 respectively), indicating robust overall performance across these different datasets. Overall, MedViT achieves the top two highest ACC in 10 out of the 12 data categories and the top two highest AUC in 9 out of the datasets. It demonstrates high effectiveness on these medical imaging datasets, especially for PathMNIST, PneumoniaMNIST, and BloodMNIST, with consistently high AUC and ACC scores, indicating strong predictive performance and reliability. It would be a good choice for tasks similar to those datasets where high sensitivity and specificity are crucial.

Table 2 illustrates the training results of MedViT on RetinaMNIST with different hyperparameters  $\alpha$  after replacing the loss function with Ordinal Loss. Here,  $\alpha=0.0$  corresponds to using only the original cross-entropy loss function. It can be observed that as  $\alpha$  increases, the weight of the Rank Loss increases, and the training performance shows a trend of improvement followed by deterioration. At  $\alpha=0.2$ , the model achieves the best performance, with a significant improvement of 4% compared to the original, reaching an accuracy close to 60%. This

indicates that Ordinal Loss indeed effectively enhances MedViT's performance in ordinal regression tasks. Moreover, the proportion of Rank Loss should not be maximized; instead, it needs to be balanced with traditional cross-entropy to achieve optimal performance.

Table 2: Performance of MedViT with Ordinal Loss on RetinaMNIST.

$\alpha$	0.0	0.1	0.2	0.3	0.4	0.5
ACC	0.552	0.570	0.594	0.581	0.557	0.546

Figure 4 shows the attention heatmap of two models trained using the traditional loss function and  $\alpha=0.2$  Ordinal Loss, respectively, when identifying samples from two adjacent classes. The retinal image above corresponds to a lesion severity level of 1, while the one below corresponds to level 2. The green boxes highlight the areas of significant retinal lesions, which serve as the primary discriminative features. The deeper red regions in the heatmap indicate areas that play a more significant role in the model's classification process. It can be observed that in the heatmap of the model trained with Ordinal Loss, the red regions overlap more closely with the green boxes, indicating that this model better captures the key features for distinguishing between samples from two adjacent classes. In contrast, in the heatmap of

the model trained with traditional cross-entropy loss, the red regions are concentrated mainly in the middle of the image, failing to effectively differentiate between the two classes of samples. The experimental results and visual inspection demonstrate that as expected, Ordinal Loss enables the model to better distinguish between adjacent classes, thus improving the performance on ordinal regression tasks.

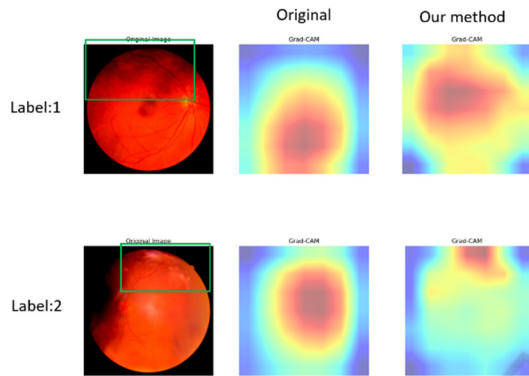


Figure 4: Visual inspection of models trained with two different loss functions using GradCAM (Photo/Picture credit: Original).

## 4 CONCLUSIONS

This study concentrates on utilizing transformer models for image classification tasks on MedMNIST and enhancing the performance of ordinal regression subtasks using a novel loss function. The MedViT model, a hybrid architecture combining CNN and transformer, is employed to classify all 12 2D datasets in MedMNIST and compared against classical CNN models. Experimental findings reveal that MedViT, adept at capturing multi-scale features, showcases significant advantages over traditional methods, yielding superior performance across most of the 12 datasets. The development of Ordinal Loss aims to address the observed performance limitations across all models on the ordinal regression subdataset, RetinaMNIST. This loss function combines traditional cross-entropy loss with Rank Loss, emphasizing similarity relationships between ordered categories during model training. Comparative experiments with unmodified cross-entropy loss demonstrate that models trained with Ordinal Loss achieve higher accuracy on RetinaMNIST for ordinal regression tasks. Visual inspection using GradCAM further illustrates that Ordinal Loss enables the model to better discern key features for distinguishing adjacent categories. In the realm of fine-grained

recognition, certain methods enhance model performance by learning pairs of intra-class and inter-class similar samples. In future research, this approach could also be considered for integration into the ordinal regression task to further enhance the model's ability to discern similar samples effectively.

## REFERENCES

- Dosovitskiy, A., Beyer, L., Kolesnikov, A., Weissenborn, D., Zhai, X., Unterthiner, T., ... & Houshy, N. 2020. An image is worth 16x16 words: Transformers for image recognition at scale. arXiv:2010.11929.
- He, K., Zhang, X., Ren, S., & Sun, J. 2016. Deep residual learning for image recognition. In Proceedings of the IEEE conference on computer vision and pattern recognition. pp: 770-778.
- Heo, B., Yun, S., Han, D., Chun, S., Choe, J., & Oh, S. J. 2021. Rethinking spatial dimensions of vision transformers. In Proceedings of the IEEE/CVF international conference on computer vision. pp: 11936-11945.
- Hu, Q., Chen, C., Kang, S., Sun, Z., Wang, Y., Xiang, M., ... & Wang, S. 2022. Application of computer-aided detection (CAD) software to automatically detect nodules under SDCT and LDCT scans with different parameters. Computers in Biology and Medicine, vol. 146, p: 105538.
- Hu, W., Li, C., Li, X., Rahaman, M. M., Ma, J., Zhang, Y., ... & Grzegorzec, M. 2022. GasHisSDB: A new gastric histopathology image dataset for computer aided diagnosis of gastric cancer. Computers in biology and medicine, vol. 142, p: 105207.
- Lo, C. M., & Hung, P. H. 2022. Computer-aided diagnosis of ischemic stroke using multi-dimensional image features in carotid color Doppler. Computers in Biology and Medicine, vol. 147, p: 105779.
- Manzari, O. N., Ahmadabadi, H., Kashiani, H., Shokouhi, S. B., & Ayatollahi, A. 2023. MedViT: a robust vision transformer for generalized medical image classification. Computers in Biology and Medicine, vol. 157, p: 106791.
- Simonyan, K., & Zisserman, A. 2014. Very deep convolutional networks for large-scale image recognition. arXiv:1409.1556.
- Yang, J., Shi, R., Wei, D., Liu, Z., Zhao, L., Ke, B., ... & Ni, B. 2023. Medmnist v2-a large-scale lightweight benchmark for 2d and 3d biomedical image classification. Scientific Data, vol. 10(1), p: 41.
- Yang, X., & Stamp, M. 2021. Computer-aided diagnosis of low grade endometrial stromal sarcoma (LGESS). Computers in Biology and Medicine, vol. 138, p: 104874.